Statistics and Its Interface Volume 11 (2018) 491–501

Testing the zonal stationarity of spatial point processes: applied to prostate tissues and trees locations

Azam Saadatjouy, Ali Reza Taheriyoun*, and Mohammad Q. Vahidi-Asl

This work aims to test the second-order stationarity of a spatial point pattern based on the local spectra concept. Using a logarithmic transformation, the mechanism of the proposed test becomes approximately identical to a simple two factor analysis of variance with the known variance of the noise term. This procedure can be also used for testing the stationarity in the neighborhood of a particular point of the observation window. The same idea is used in post-hoc tests to cluster the point pattern into stationary and non-stationary sub-windows. The performance of the proposed method is examined through a simulation study and is then applied to a practical data. The proposed test shows a considerable empirical power and satisfactorily empirical size.

AMS 2000 subject classifications: Primary 60G55, 62M15; secondary 62F15.
Keywords and phrases: Complete covariance density function, Evolutionary periodogram, Spatial point process, Spectral density function, Zonal stationarity.

1. INTRODUCTION

1.1 General aspects

A point pattern as a realization of a point process is a set of points distributed irregularly in a window. The analysis of a point pattern provides information on the geometrical structures formed by the aggregation and interaction between points. The aggregation and interaction of points are characterized by intensity and covariance density functions, respectively. A point process is first-order stationary if its intensity function is a constant function, while it is called second-order stationary if all of its second-order characteristics (e.g., the complete covariance density function) are only a function of inter-points distances. A point process is called stationary here when it is first- and second-order stationary, simultaneously. Therefore, for a nonstationary process at least one of the first- or second-order stationarity characteristics does not hold to be true. The spectral density function of a stationary point process is the Fourier transform of the complete covariance density function. The main key point of this study is the fact that 'the structure of the complete covariance density and spectral density functions may vary with the location when the stationarity assumption is violated'.

Several efficient methods based on the spectral density are available in the literature for studying the spatial structure of stationary processes. The spectral methods have been used by [12] to investigate the asymptotic properties of several estimation methods in a stationary process observed on a d-dimensional lattice. The approximated locations of events in a spatial point pattern have been presented using the intersections of a fine lattice on the observation window by [25] and the point spectrum has been approximated by the lattice spectrum. A quick glance at the published literature shows that a considerable number of studies have been dedicated to test the stationarity problem by testing the first-order stationarity. Among the methods available, we refer to [11] for a formal test of the first-order stationarity of point processes. The proposed model-free test statistic is based on the squared deviations of observed counts of points from their expected counts under the first-order stationarity. Chiu and Liu [5] have extended this method to a general class of statistics by incorporating the information of projected points onto the axes. For testing the first-order stationarity of point processes in arbitrary regions, a Kolmogrov-Smirnove type test is proposed by [29], where the test statistic is obtained by maximizing the absolute difference between the observed and estimated counts of points.

The main interest of the statistical analysis is to evaluate the second-order characteristics of point processes when the first-order stationarity is satisfied. For this purpose, several so-called summary statistics such as Ripley's K-function [26], L-function [4] and pair correlation function [28] have been proposed.

Generally, a vague boundary exists between stationary and nonstationary point processes containing zonal stationary processes. For the zonal stationary processes, there exist natural or artificial boundaries in a space where the covariance structure changes between the boundaries but the

arXiv: 1701.08365v1
*Corresponding author.

intensity structure remains unchanged. Both the zonal stationary and stationary point processes are first-order stationary, but unlike the stationary point processes, the zonal stationary processes are not second-order stationary in the whole of observation window. However, the restriction of zonal stationary processes into some sub-regions of original window are stationary. This concept is further explained in Section 2.1. Based on a point pattern, we want to decide between the zonal stationarity and the simple stationarity assumption. One may suggest to employ methods developed for regular observation of random fields. To this end, since the point pattern is an irregular observation of points, we need to partition the observation window, $W \subseteq \mathbb{R}^d$, into a regular d-dimensional grid where the ith edge of W is divided into n_i, $i = 1, \cdots, d$, equidistant parts. Let $N_{\mathbf{i}}$ represent the number of points in the sub-cube in the $\mathbf{i}$th row, where $\mathbf{i} = (i_1, \cdots, i_d)$, and $i_j = 1, \cdots, n_j$. We evaluate the stationarity of a point pattern by testing the stationarity of the random field $\{N_{\mathbf{i}}\}_{\mathbf{i}}$. This test is similar to the test for stationarity of random fields introduced by [10] but looses the information about the locations of points. In the second approach, we define the evolutionary spectra for the realization of a point process and then examine the local behavior of the discrete evolutionary spectra. The stationarity assumption is rejected if the spectral density function shows different behavior at least in two different regions of the observation window. We mention the property of different behaviors in different regions by *second-order location dependency*. Our method is designed to detect the second-order stationarity against this behavior.

The concept of evolutionary (i.e. time-dependent) spectra of random processes has been introduced by [22, 21]. Testing the stationarity of time series is a very famous consequence of this concept [24]. Using the time-dependent spectra, the asymptotic properties of nonstationary time series with locally stationary behavior have been investigated by [6]. The remaining references somehow have used the evolutionary or local spectra for testing the stationarity of regular trajectories of random fields except [2] that has proposed a test for spatial stationarity based on a transformation of irregularly spaced spatial data. Nonparametric and several parametric procedures for modeling the spatial dependence structure of a nonstationary spatial process observed on a d-dimensional lattice have been proposed by [9]. Priestley's idea has been extended to test the stationarity and isotropy of a spatial process [10].

This paper is organized as follows: In the sequel, we study two motivating datasets. In the following section, we review some concepts of point processes and present two spatial spectral representations for a nonstationary spatial point process. Moreover, the nonparametric estimates of the spectral density of a nonstationary point process are proposed in this section. A formal test of the second-order stationarity is presented in Section 3. In Section 4, we examine the proposed testing approach through a simulation study. We also study the effect of location in the competition between a specific genus of trees in 4.1.

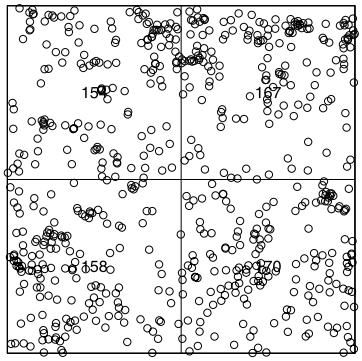

Figure 1. The locations of 649 *trees of the Bar Colorado forest in a rectangular window whose vertices are located at the geographic coordinates* $(500, 0)$ *and* $(700, 333/3333)$. *The sampling window is rescaled into* $[0, 70]^2$.

1.2 Data and motivations

In this section, we propose two datasets and motivations for their analysis in order to illustrate the mentioned problem comprehensively. The first dataset is devoted to the location of *Euphorbiaceae* trees in a part of the Bar Colorado forest (Figure 1). We will discuss the sub-windows of this figure in Sections 2.1 and 4.1. Generally, one of the main and essential information for forest management and its optimal and sustainable utilization is to determine the frequencies of different types of trees, distribution pattern of trees, and their competition. For example, the distribution of trees seeds could have an impact on their aggregation while competition among different species for moisture, light, and nutrients acts oppositely. A positive autocorrelation or aggregation may result from regeneration near parents, whilst a negative autocorrelation results from their competition. Therefore, it seems that variations of the aggregation structure will change the interaction structure of trees. Since the local periodogram is influenced by the aggregation and interactions of points, so we use this function to detect the location(s) at which the pattern of trees distribution is changed.

The second data is the location of capillary profiles on a section of prostate tissue. According to the anatomy of the human body, blood circulation in the human body starts from the heart, then flows through arteries, and finally receives to all parts of the body by capillaries. Capillaries are the smallest vessels of the body, supplying the oxygen to tissues and exchanging constituents between tissues and blood. Figure 2 demonstrates the midpoints of the capillaries in sections of a healthy and a cancerous prostate tissues. The rescaled point patterns published by [13] have been used to capture the coordinates of the capillaries. Since the quantity of nutrients and oxygen required by different parts of a given

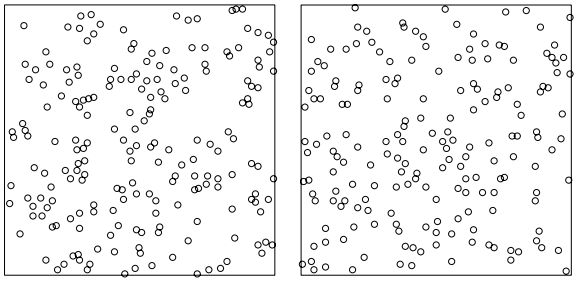

(a) healthy tissue (b) cancerous tissue

Figure 2. The locations of 196 *capillaries on a section of a healthy prostate (2a) and the locations of* 185 *capillaries at the same section from a cancerous prostate (2b).*

organ of the body are not same, so it is expected that the density of capillary network will be different in various parts of the body. In order to scrutinize this issue, we examine the behavior of evolutionary periodogram function at different parts of a tissue.

2. NONSTATIONARY SPECTRAL APPROACHES

2.1 Preliminaries and notations

Let X be a spatial point process observed within the bounded region $W \subseteq \mathbb{R}^d$. The first- and second-order intensities are used to determine the aggregation and dependency structure of the point patterns. The first-order intensity function is defined as the expected number of points per unit volume [7, page 43] in the following way:

$$\lambda_X(\mathbf{a}) = \lim_{|\mathrm{d}\mathbf{a}|\to 0} \frac{\mathbb{E}[N_X(\mathrm{d}\mathbf{a})]}{|\mathrm{d}\mathbf{a}|}, \qquad \mathbf{a} \in \mathbb{R}^d,$$

where $d \in \mathbb{N}$, $\mathrm{d}\mathbf{a}$ is an infinitesimal region around the point $\mathbf{a}$, $|\mathrm{d}\mathbf{a}|$ is the volume of this region, and $N_X(\mathrm{d}\mathbf{a})$ is the number of points of X in this small region. The second-order intensity, λ_{XX}, contains information about the stochastic dependence of points in two different regions [7, page 43]; that is

$$\lambda_{XX}(\mathbf{a},\mathbf{b}) = \lim_{|\mathrm{d}\mathbf{a}|,|\mathrm{d}\mathbf{b}|\to 0} \frac{\mathbb{E}[N_X(\mathrm{d}\mathbf{a})N_X(\mathrm{d}\mathbf{b})]}{|\mathrm{d}\mathbf{a}||\mathrm{d}\mathbf{b}|},$$

for any $\mathbf{a},\mathbf{b} \in \mathbb{R}^d$ such that $\mathbf{a} \neq \mathbf{b}$. Bartlett [3] proposed the unit-free complete covariance density function, κ_{XX}, defined by

$$\begin{aligned}\kappa_{XX}(\mathbf{a},\mathbf{b}) &= \lambda_X(\mathbf{a})\delta(a_1-b_1)\delta(a_2-b_2)\ldots\delta(a_d-b_d)\\ &+ \gamma_{XX}(\mathbf{a},\mathbf{b}),\end{aligned}$$

where $\delta(a)$ is the Dirac delta function and γ_{XX} is the covariance density function, which in turn is defined by

$$\begin{aligned}\gamma_{XX}(\mathbf{a},\mathbf{b}) &= \lim_{|\mathrm{d}\mathbf{a}|,|\mathrm{d}\mathbf{b}|\to 0} (|\mathrm{d}\mathbf{a}||\mathrm{d}\mathbf{b}|)^{-1}\\ &\times \mathbb{E}\left[(N_X(\mathrm{d}\mathbf{a}) - \lambda_X(\mathrm{d}\mathbf{a}))\,(N_X(\mathrm{d}\mathbf{b}) - \lambda_X(\mathrm{d}\mathbf{b}))\right]\\ &= \lambda_{XX}(\mathbf{a},\mathbf{b}) - \lambda_X(\mathbf{a})\lambda_X(\mathbf{b}).\end{aligned}$$

A point process is called stationary if its distribution is invariant under translations. It is called isotropic if its distribution is invariant under rotations about the origin in $\mathbb{R}^d$. For a stationary point process, the intensity function is constant and the second-order characteristics depend only on the lag vector. Moreover, for an isotropic process such dependency is an exclusive function of the scalar length of lag vector regardless of the orientation. Moving to the frequency domain approaches, the spectral density function of a point process is the Fourier transform of the complete covariance density function. It is a function like $\mathrm{f}_{XX} : \mathbf{\Omega} \longrightarrow \mathbb{C}$, where $\mathbf{\Omega}$ is the space of frequencies defined as (see [20]) the Fourier transform of the unit-free complete covariance density function, κ_{XX} [3]. For a nonstationary spatial process, Fuentes [10] generalized the evolutionary spectra concept of time series introduced by [22]. Following the same idea, we introduce two different evolutionary periodograms of nonstationary point processes. A new class of nonstationary point processes called 'zonal' stationary processes is introduced. In each approach, an empirical spectral density function is defined for this class whose physical interpretation is similar to that of the spectrum of a stationary point process, but it varies with location. Intuitively, a point process is called zonal stationary if it behaves in an approximately stationary way in several disjoint sub-regions. The formal definition of the zonal stationary point process is as follows:

Definition 2.1. A first-order stationary point process X is called zonal stationary on $W \subseteq \mathbb{R}^d$ if there exists a partition $(W_1,\ldots,W_k)$ for W such that $\exists r_i^\star > 0, \forall r_i > r_i^\star$, $X_{W_i \ominus r_i}$ are second-order stationary for all $i = 1,\ldots,k$, where $W_i \ominus r_i = \{\xi \in W_i : b(\xi, r_i) \subseteq W_i\}$.

In the definition above, X_A denotes the restriction of X to set A and $b(\xi, r)$ shows a closed ball centered at ξ with a radius r. Furthermore, the minus-sampling method is used to handling edge effects [19, page 39]. In this method, all the boundary regions are excluded and only those regions lying entirely inside the observation window are sampled. The first-order intensity functions of $X_{W_i}, i = 1,\ldots,k$, are equal to constant λ in each sub-region ($\lambda_{X_{W_i}}(\mathbf{a}) = \lambda,\ \mathbf{a} \in \mathbb{R}^d$). The second-order intensity functions of $X_{W_i}, i = 1,\ldots,k$, are only functions of lag vector in each sub-region but vary from one sub-region to another ($\lambda_{X_{W_i}X_{W_i}}(\mathbf{a},\mathbf{b}) = \lambda_{X_{W_i}X_{W_i}}(\mathbf{a}-\mathbf{b});\ \mathbf{a},\mathbf{b} \in \mathbb{R}^d$).

Note 2.1. *There exists an edge effect at the boundaries of each W_i. For regular W_i, we assume that $\gamma_{X_{W_i}X_{W_i}}(\|h\|) = o(\|h\|^\epsilon)$, where $\epsilon > 1$ is chosen such that the interaction of far points in comparison with diameter of W_i is negligible. Note also that this is not a big concern since for the first-order stationary processes the complete covariance density function is equal to $\lambda\delta_0 + \lambda^2(g-1)$ where g is the paired*

correlation function and δ_0 is Dirac's delta. Therefore, the mentioned assumption is the consequence of the convergence behavior of $g(\mathbf{a})$ when $\|\mathbf{a}\| \to \infty$. The simple examples to study this behavior are Hawkes process [14], Log Gaussian Cox process [19, Page 72] and χ^2 Cox process [19, Page 76].

Creating appropriate partitions, the number of disjoint sub-regions, and identifying their shapes have a great importance on analyzing zonal stationary processes. For analyzing locally stationary random fields, [8] have postulated that the shape of the sub-regions are known a priori and the number of sub-regions is estimated using the Akaike information criterion. A Voronoi tessellation has been employed to construct the sub-regions in [16]. The regional behavior of a point pattern can be detected through evaluating its different features in the special regions. In this article we propose a new method for partitioning the spatial domain into disjoint sub-windows in which the restricted point patterns are assumed to be stationary. It is worth mentioning that sub-regions refer to subsets of the original observation window within which local stationary point patterns are observed. These areas do not have necessarily regular shapes. However, 'sub-windows' refer to regular square areas used throughout this study to partition the observation window. Figure 3a shows the observation window of a zonal stationary point pattern such that the observed local point patterns in each of the shaded connected sub-regions are stationary. Firstly, the observation window is partitioned to 2^2 identical square-shaped sub-windows. The shape of sub-windows are considered to be square for independence of the periodograms [see 1, for details]. Our computation in each sub-window is weighted (according to a regular weight function) in a closed ball centered at the middle point of the sub-window. This type of computation does not use the points located near the boundaries, it is neither affected by the edge effect nor the hard interaction of neighbor sub-regions onto these points. Accordingly, the stationarity is examined through these balls. Secondly, the number of regular partitions is increased in such a way that: 1) the asymptotic results about the local spectra hold to be true by mean that the number of points in each sub-window must be large enough and the diameter of sub-windows are not smaller than a specific value, 2) *and* the stationarity assumption satisfied in each sub-window, 3) *or* it is verified that the second-order properties of at least two sub-windows are different. This issue is shown in Figure 3b and 3c. Determination of sub-regions is a nonparametric problem since the dimension of parameter space is uncountable. In practice and for simplification, the nonparametric estimation problem is replaced with the parametric testing by assuming that different local stationary point patterns are observed in regular sub-regions. Although determining these regions is crucial in the spatial domain, this issue can be easily solved in the frequency domain due to its independency from the observation window. This could be attributed to the fact that the frequency domain is based on $[-\pi, \pi]$ regardless of the

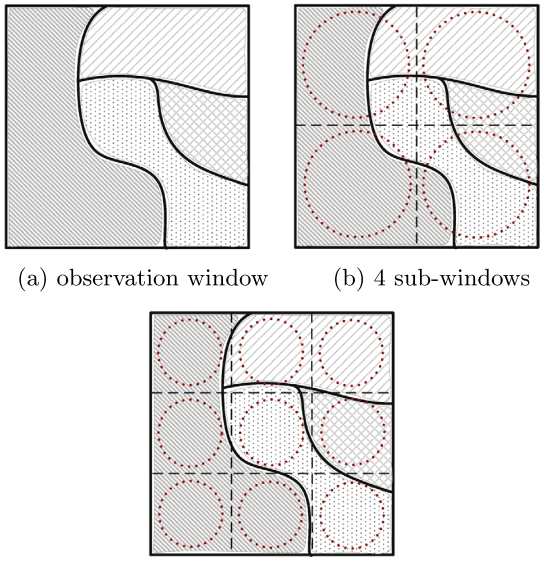

(a) observation window (b) 4 sub-windows

(c) 9 sub-windows

Figure 3. Determination of sub-windows for a realization of zonal stationary point process.

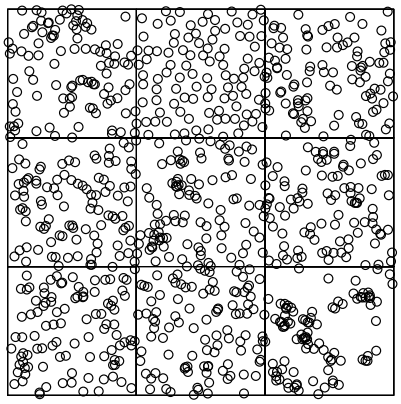

Figure 4. A realization of the zonal stationary point process.

form of the observation window. The Bartlett window can be used to determine different regions on which the features must be evaluated and, accordingly, the regional behavior of the point pattern can be detected by computing the local periodogram.

Figure 4 shows a realization of a zonal stationary point process in the window $W = [0, 70]^2$. The local point patterns are generated independently here in regular sub-regions. We term $\mathbf{z}_1, \ldots, \mathbf{z}_9$ the middle points of $\mathbf{S}_1, \ldots, \mathbf{S}_9$ square sub-regions from left to right and down to up, respectively. In this figure, the point patterns in $\mathbf{S}_3$ and $\mathbf{S}_8$ are realizations of the stationary Thomas process and the Simple Sequential Inhibition (SSI) process, respectively, while the remaining are realizations of the stationary Poisson processes. This point pattern is denoted by y.

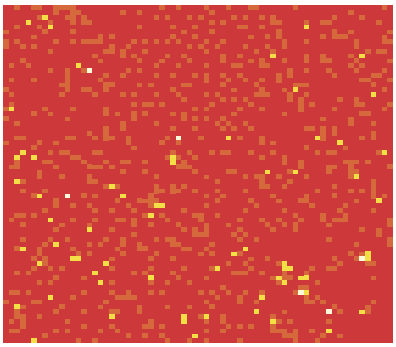

Figure 5. The regular realization of the $N_{\mathbf{i}}$ random field corresponding to the mentioned point pattern in Figure 4.

Suppose that we have a point process X observed on a rectangular window $W = [\mathbf{0}, \mathbf{l}] \subseteq \mathbb{R}^d$, where $\mathbf{l} = (l_1, \ldots, l_d)$, that is the rectangular window with a vertex at the origin of the Cartesian system and an opposite vertex on $\mathbf{l}$. Construct $\{N_{\mathbf{i}}\}_{\mathbf{i}}$ as explained previously. We consider a regular $n_1 \times \ldots \times n_d$ grid on the study area and set $n = \prod_{j=1}^{d} n_j$. Let $N_{\mathbf{i}}$ be the number of points in the sub-cube with vertex $\mathbf{i} = (i_1, \ldots, i_d)$, $i_j = 1, \ldots, n_j$ for $j = 1, \ldots, d$. We define the random field as $V(\mathbf{s}) = N_{\mathbf{i}}$ if $\mathbf{s}$ belongs to the sub-cube $\mathbf{i}$. Figure 5 shows the image of $N_{\mathbf{i}}$ random field obtained from the point pattern presented in Figure 4. Now, one may use the method of [10] to define the local periodogram of the obtained random field. This approach eliminates the information of the location of points and hence we propose another approach based on the nonstationary periodogram.

2.2 Nonstationary periodogram of point processes

Assume that we have a point pattern x observed on a rectangular window $W = [\mathbf{0}, \mathbf{l}] \subseteq \mathbb{R}^d$ containing n_X points. Let $D = \{\mathbf{u}_j = (u_{1j}, \ldots, u_{dj}), j = 1, \ldots, n_X\}$, be the set of positions of the points. Suppose the approximate locations of points in a point pattern be represented by the intersections of a $m_1 \times \ldots \times m_d$ fine lattice superimposed on the study region. This lattice generates an irregular realization of a binary random field $\{\zeta(\mathbf{s})\}$ as

$$\zeta(\mathbf{s}) = \begin{cases} 1 & \text{if } \mathbf{s} \in D \\ 0 & \text{if } \mathbf{s} \notin D. \end{cases}$$

$\zeta(\mathbf{s})$ is a simple random field and it only considers the positions of points occurrence. There is an equivalence between the point spectra of X and the spectra of the random field ζ [25]. If X is a stationary point process, then ζ will be a stationary random field. Consequently, any evidence of nonstationarity of ζ could be a reason for rejection of the stationarity hypothesis of X. Suppose that ζ be zonal stationary, then its spectral density function, denoted by $f_{\mathbf{z}}(\boldsymbol{\omega})$, is the Fourier transform of the locally auto covariance function of ζ and $\mathbf{z}$ is the location around that ζ behaves stationarily ([see 10]). If for a given $\mathbf{z}$ the function $f_{\mathbf{z}}(\boldsymbol{\omega})$ is not sensitive to $\boldsymbol{\omega}$, then we conclude that in the neighborhood of the given $\mathbf{z}$, $f_{\mathbf{z}}(\boldsymbol{\omega})$ belongs to a completely spatial random point pattern. On the other hand, if for a given frequency $\boldsymbol{\omega}$, $f_{\mathbf{z}}(\boldsymbol{\omega})$ is not sensitive to $\mathbf{z}$, then we conclude that for the given $\boldsymbol{\omega}$, $f_{\mathbf{z}}(\boldsymbol{\omega})$ does not behave locally. Practically, $f_{\mathbf{z}}(\boldsymbol{\omega})$ is unknown for every $\mathbf{z}$ and for every $\boldsymbol{\omega}$ and we restrict the problem of estimation to specific Fourier frequencies and locations. Therefore, our approach is a parametric statistical inference.

Consider a location varying filter to assign greater weights to the neighboring values of $\mathbf{z}$. The spatial local periodogram at a location $\mathbf{z}$ and frequency $\boldsymbol{\omega}$ is $|\mathcal{J}_{\mathbf{z}}(\boldsymbol{\omega})|^2$, where

$$\begin{aligned} \mathcal{J}_{\mathbf{z}}(\boldsymbol{\omega}) &= \frac{1}{\sqrt{\prod_{j=1}^{d} l_j}} \sum_{k=1}^{m} g(\mathbf{z} - \mathbf{s}_k)\zeta(\mathbf{s}_k) \exp\{-i\mathbf{s}_k^T\boldsymbol{\omega}\} \\ &= \frac{1}{\sqrt{\prod_{j=1}^{d} l_j}} \sum_{j=1}^{n_X} g(\mathbf{z} - \mathbf{u}_j) \exp\{-i\mathbf{u}_j^T\boldsymbol{\omega}\} \\ &= A_{\mathbf{z}}(\boldsymbol{\omega}) + iB_{\mathbf{z}}(\boldsymbol{\omega}), \end{aligned} \tag{1}$$

where $g : \mathbb{R}^d \to \mathbb{R}$ is the filter function with all the characteristics mentioned by [10] with finite width B_g defined as $B_g = \int_{\mathbb{R}^d} ||\mathbf{u}||g(\mathbf{u})\mathrm{d}\mathbf{u}$, and $m = m_1 \times \ldots \times m_d$. The resulting periodogram is not smooth enough to be used as an estimation of the local spectra and, thus, $|\mathcal{J}_{\mathbf{z}}|^2$ is smoothed using the $\mathbb{L}^2$ kernel family, $\{W_\rho\}$, where for each ρ there exists a constant C such that

$$\lim_{\rho \to \infty} \rho^d \int_{\mathbb{R}^d} |w_\rho(\lambda)|^2 \mathrm{d}\lambda = C, \tag{2}$$

where w_ρ is the Fourier transform of W_ρ. Thus, the final estimator is

$$\widehat{f}_{\mathbf{z}}(\boldsymbol{\omega}) = I_{\mathbf{z}}(\boldsymbol{\omega}) = \int_{\mathbb{R}^d} W_\rho(\mathbf{z} - \mathbf{u})|\mathcal{J}_{\mathbf{z}}(\boldsymbol{\omega})|^2 \mathrm{d}\mathbf{u}. \tag{3}$$

Analogous to [10], the covariance between the spatial periodogram values $I_{\mathbf{z}_1}(\boldsymbol{\omega})$ and $I_{\mathbf{z}_2}(\boldsymbol{\omega}')$ will be asymptotically zero if either $\|\boldsymbol{\omega} \pm \boldsymbol{\omega}'\| \gg$ bandwidth of $|\Gamma(\boldsymbol{\theta})|^2$ where Γ is the Fourier transform of g and $\|\mathbf{z}_1 \pm \mathbf{z}_2\| \gg$ bandwidth of the function $W_\rho(\mathbf{u})$ [23]. For fixed $\mathbf{z}$ and $\boldsymbol{\omega}$, one may conclude the normality of $A_{\mathbf{z}}(\boldsymbol{\omega})$ and $B_{\mathbf{z}}(\boldsymbol{\omega})$ similar to the [20]. There is no certain criterion in the literature for the required number of points to obtain the asymptotic normality of $A_{\mathbf{z}}(\boldsymbol{\omega})$ and $B_{\mathbf{z}}(\boldsymbol{\omega})$. In fact, this criterion does not exist even for the global version of A and B which are not dependent to the locations, $\mathbf{z}$. But our simulation study showed that when the number of points in each sub-window exceeds 50, the asymptotic normality is well-satisfied.

Figure 6 shows the spatial local periodogram of the mentioned y in Figure 5 at the Fourier frequencies and at the locations $\mathbf{z}_1, \ldots, \mathbf{z}_9$ which are enough wide apart. The number of observed points of y in the considered sub-windows are almost similar. Obviously, as shown in Figure 6, the behavior of the local periodogram function of y varies at

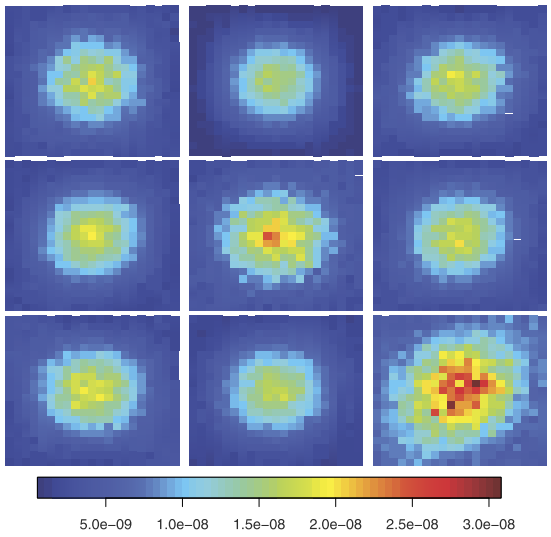

Figure 6. The spatial local periodogram of the point pattern of Figure 4 at the locations $\mathbf{z}_1, \ldots, \mathbf{z}_9$ and Fourier frequencies.

different locations. The shape of the local periodograms in sub-windows with stationary Poisson patterns (around $\mathbf{z}_k$, $k \in K = \{1, 2, 4, 5, 6, 7, 9\}$,) are broadly flat, reflecting the absence of the interaction structure in the observed patterns. In the sub-window with the stationary Thomas pattern, for small values of $\|\boldsymbol{\omega}\|$ the values of $I_{\mathbf{z}_3}(\boldsymbol{\omega})$ are larger in comparison with $I_{\mathbf{z}_j}(\boldsymbol{\omega})$ when $j \in K$. In contrast, for the sub-window with the Simple Sequential Inhibition pattern, the values of $I_{\mathbf{z}_8}(\boldsymbol{\omega})$ are smaller than $I_{\mathbf{z}_j}(\boldsymbol{\omega})$, $j \in K$, when $\|\boldsymbol{\omega}\|$ is small.

There is a fundamental difference between this location dependent point spectra and the lattice-based local spectra considered by [10]. A lattice-based spectrum describes the spatial structure of a measured variable (i.e., tree heights) at fixed equally spaced locations in an $n_1 \times n_2$ grid. However, in a local point spectrum, we consider the spatial structure of the location (for example, locations of trees) of points instead of a measured characteristic. Moreover, the first estimator ignores the information about the precise locations of points compared with the second one.

Concerning the Bartlett's window, $g(\mathbf{u})$ is considered as a multiplicative filter in the simulation study of Section 4; i.e. $g(\mathbf{u}) = \prod_{j=1}^{d} g_1(u_j)$, where $g_1(u) = (4\pi h)^{-1/2}\mathbf{1}_{|u|\le h}$. Thus, the Fourier transform of g becomes $\Gamma(\boldsymbol{\omega}) = \prod_{j=1}^{d}(\sqrt{h\pi}\omega_j)^{-1}\sin(h\omega_j)$. In addition, we consider $W_\rho(\mathbf{u})$ to be of the form $W_\rho(\mathbf{u}) = \prod_{j=1}^{d} W_{1,\rho}(u_j)$, where $W_{1,\rho}(u) = 1/\rho\mathbf{1}_{|u|\le\rho/2}$, corresponding to the Daniell window, implies the accuracy of formula (2) with $C = (2\pi)^d$.

3. TESTING THE STATIONARITY

In this section, we represent a formal test of stationarity of a point process based on the arguments presented in the previous section. The analysis of the geometric structure of a point pattern is strongly related to the aggregation of points and interaction between points. When the aggregation of points is the same at two different sub-windows, it is not easy to visually discriminate the interaction effect in these sub-windows. In this situation, the higher moments of the point pattern such as the second-order intensity function must be compared together in different areas. If the restricted point patterns to disjoint sub-windows are assumed to be independent, their second order properties can be compared according to [27]. Without such independency, *two-factor analysis of variance* model and following assumptions are valid. We thus write (see also [15, 24])

$$Y(\mathbf{z}, \boldsymbol{\omega}) = \ln I_{\mathbf{z}}(\boldsymbol{\omega}) = \ln f_{\mathbf{z}}(\boldsymbol{\omega}) + \varepsilon(\mathbf{z}, \boldsymbol{\omega}). \tag{4}$$

Priestley and Subba Rao [24] have showed that asymptotically $\mathbb{E}[\varepsilon(\mathbf{z}, \boldsymbol{\omega})] = 0$ and

$$\sigma^2 = \mathbb{E}[\varepsilon(\mathbf{z}, \boldsymbol{\omega})]^2 = \left(C/\rho^2\right) \int_{\mathbb{R}^d} |\Gamma(\boldsymbol{\theta})|^4 \mathrm{d}\boldsymbol{\theta}, \tag{5}$$

for $\boldsymbol{\omega} \notin \delta\Pi_\Delta^d$, where $\Pi_\Delta^d = [-\pi, \pi]^d$ and $\delta\Pi_\Delta^d$ denotes the boundary of the region Π_Δ^d.

We select a set of locations $\mathbf{z}_1, \mathbf{z}_2, \ldots, \mathbf{z}_m$ and a set of frequencies $\boldsymbol{\omega}_1, \boldsymbol{\omega}_2, \ldots, \boldsymbol{\omega}_n$ in such a way that an acceptable sample is gathered in location and frequency spaces. $I_{\mathbf{z}}(\boldsymbol{\omega})$ is evaluated over this fine sample. The set of locations and frequencies must also be wide apart enough in order to $\varepsilon(\mathbf{z}_i, \boldsymbol{\omega}_j)$ and consequently $I_{\mathbf{z}_i}(\boldsymbol{\omega}_j)$ be uncorrelated. If we write $Y_{ij} = Y(\mathbf{z}_i, \boldsymbol{\omega}_j)$, $f_{ij} = \ln f_{\mathbf{z}_i}(\boldsymbol{\omega}_j)$ and $\varepsilon_{ij} = \varepsilon(\mathbf{z}_i, \boldsymbol{\omega}_j)$, then using the discussion on the normality of $A_{\mathbf{z}}$ and $B_{\mathbf{z}}$, the noise terms, ε_{ij}, are considered to be normally distributed and Y_{ij} are generated according to the model

$$Y_{ij} = f_{ij} + \varepsilon_{ij}.$$

The parameter f_{ij} represents the treatment effect of both the location at level $\mathbf{z}_i$ and the frequency at level $\boldsymbol{\omega}_j$. By considering the normality of the main effects, we can rewrite the model as

$$\begin{aligned} &H_1 : Y_{ij} = \mu + \alpha_i + \beta_j + \gamma_{ij} + \varepsilon_{ij}, \\ &\quad i = 1, \ldots, m \quad \text{and} \quad j = 1, \ldots, n. \end{aligned} \tag{6}$$

In this model, the parameters α_i and β_j represent the main effects of the location and frequency factors, respectively, and γ_{ij} represents the interaction between these two factors. As previously mentioned, the spectral density function of a stationary point process does not oscillate locally and it only varies by change of the frequencies. Therefore, the stationarity of a point process can be tested by using the analysis of variance methods and testing the model

$$H_0 : Y_{ij} = \mu + \beta_j + \varepsilon_{ij}, \ i = 1, \ldots, m \quad \text{and} \quad j = 1, \ldots, n,$$

or equivalently $H_0 : \alpha_i = 0$, $i = 1, \ldots, m$, versus (6). The rejection of H_0 represents that at least one of the parameters

α_i is not zero meaning that there exist at least two locations $\mathbf{z}_i, \mathbf{z}_j \in W$ in such a way that $f_{\mathbf{z}_i}(\boldsymbol{\omega}) \neq f_{\mathbf{z}_j}(\boldsymbol{\omega})$. A post-hoc test is used to find different location(s) and thus we may use this as a clustering method in the zonal stationary point processes. Since the value of $\sigma^2 = \mathbb{V}ar(\varepsilon_{ij})$ is known, the presence of the interaction factor, γ_{ij}, can be tested only using one realization of a given point process. If the effect of interaction factor is not significant, then the point process is uniformly modulated and $\ln f_{\mathbf{z}}(\boldsymbol{\omega})$ will be additive in terms of location and frequency. We can examine whether the nonstationarity of the point pattern is restricted only to some frequencies by testing for stationarity over these frequencies. If X is an isotropic point process, then $f_{\mathbf{z}}(\boldsymbol{\omega})$ depends on its vector argument $\boldsymbol{\omega}$ only through its scalar length $\|\boldsymbol{\omega}\|$, regardless of the orientation of $\boldsymbol{\omega}$. Then, we can test for isotropy by selecting a set of frequencies with the same norms, say $\{\boldsymbol{\omega}_{j_1}, \boldsymbol{\omega}_{j_2}\}$ where $\boldsymbol{\omega}_{j_1} \neq \boldsymbol{\omega}_{j_2}$ but $\|\boldsymbol{\omega}_{j_1}\| = \|\boldsymbol{\omega}_{j_2}\|$, and test whether the frequency effect is significant. Since σ^2 is known, all of these comparisons are based on a χ^2 rather than F-test.

4. SIMULATION STUDY

In this section, we evaluate the performance of the proposed test for detecting the zonal stationarity of a point process. As mentioned in the previous section, using a logarithmic transformation, the mechanism of the test is almost identical to that of a two-factor analysis of variance.

In testing for stationarity and for a given number of subwindows, firstly we consider the interaction sum of squares. If the interaction is not significant, we conclude that the point process is a uniformly modulated process and the stationarity test is continued by evaluating the 'between spatial locations' sum of squares. If the interaction sum of squares turns out to be significant, we conclude that the point pattern is nonuniformly modulated and nonstationary. Afterwards, we are going to investigate whether the source of nonstationarity is the zonal behavior or not. This is equivalent to the significant sum of squares of the location factor.

We set the nominal level of test at 0.05 and assume that all of the point processes are observed on a rectangular window $W = [0, 70]^2$. Using (1), for all cases, we estimate $f_{\mathbf{z}}(\boldsymbol{\omega})$ in which $g(\mathbf{u})$ and $W_\rho(\mathbf{u})$ employ $h = 3$ and $\rho = 20$, respectively. The bandwidth of $|\Gamma(\omega_1)|^2$ is approximately π/h. The window $W_\rho(\mathbf{u})$ has a bandwidth of ρ. Thus, the space between locations, $\mathbf{z}_i$, and frequencies, $\boldsymbol{\omega}_j$, must be at least 20 and $\pi/3$, respectively, in order to obtain approximately uncorrelated estimates. For 9 sub-windows, the points $\mathbf{z}_i$ are chosen as $\mathbf{z}_i = (z_{i_1}, z_{i_2}) = (70i_1/6, 70i_2/6)$ with $i_1, i_2 = 1, 3$ and 5, corresponding to a uniform spacing of 70/3 (just exceeding $\rho = 20$). Using the same reason to make independent estimates, we need that the distance between frequencies exceeds $\pi/3$. Thus, let $\boldsymbol{\omega}_j$ be in form of $(j_1\pi/20, j_2\pi/20)$ for $j_1, j_2 = 1, 8$ and 15. Using (5), the value of σ^2 is calculated as $\sigma^2 = 16h^2/(9\rho^2) = 0.04$. For the considered set of locations and frequencies, the degree of freedom for 'between spatial locations', 'between frequencies' and 'residual+ interaction' effects are $df_L = 8$, $df_F = 8$ and $df_{IEr} = 64$, respectively and correspondingly we denote 'between spatial locations', 'between frequencies' and 'residual+ interaction' sum of squares with SSL, SSF and $SSIEr$. In the analysis of variance table, we first evaluate the significance of the interaction effect. If $SSIEr/\sigma^2 > \chi^2_{64}(0.05)$, we conclude that the point pattern is nonstationary and nonuniformly modulated. If the interaction is not significant, we conclude that the point pattern is a uniformly modulated process, and the stationarity versus the zonal stationarity test is proceeded by comparing SSL/σ^2 with $\chi^2_8(0.05)$. Significance of the location effect suggests that the point pattern is nonstationary. Similarly, in order to evaluate between frequencies effect, SSF/σ^2 is compared with $\chi^2_8(0.05)$ and the significance of test confirms that the spectra is nonuniform.

In the following study, we simulate 1,000 realizations of stationary and zonal stationary point processes to study the empirical size and power of the proposed test. Table 1 shows the ratios of rejections of H_0. The ratios of rejections for the realizations of stationary processes represent the empirical size and the ratios of rejections for the realizations of zonal stationary processes represent the empirical power of the test. We consider realizations of the Thomas process because its clustered behavior makes it similar to a zonal stationary process. To simulate a Thomas process of the parameter (δ, τ, μ), the 'parent' point process is firstly generated according to a stationary Poisson point process of intensity δ in the study region. Then, each parent point is replaced independently by 'offspring' points which the number of offspring points of each parent is generated according to a Poisson distribution with mean μ. Finally, the position of each offspring relative to its parent location is determined by a bivariate normal distribution centered at the location of parent with covariance matrix $diag(\tau^2, \tau^2)$. The process is denoted by $T(\delta, \tau, \mu)$ and the expected number of observed points is an increasing function of δ. We also consider the realizations of stationary Poisson processes of intensity λ, denoted by $P(\lambda)$. The results of Table 1 show that the empirical size of test decreases for the larger values of δ and approaches the nominal level. The great values of empirical size are due to the use of asymptotic normal distribution for Y_{ij}. In fact, this asymptotic behavior is valid for a large enough number of points at each grid. For different realizations of stationary Poisson processes, the empirical size is zero except for $P(20)$. For the point pattern y (demonstrated in Figure 4), the point pattern in $\mathbf{S}_3$ is a realization of the stationary Thomas process with parameters $\delta = 0.046$, $\tau = 1$ and $\mu = 4$, and the point pattern in $\mathbf{S}_8$ is a realization of the SSI process with Inhibition distance $r = 1.5$. The point patterns in the other sub-windows are realizations of the stationary Poisson processes with intensity 0.184.

To simulate a SSI process with Inhibition distance r, points are added one-by-one. Each new point is generated according to the uniform distribution in the window independent from previous points. If the distance between the

Table 1. The rejections ratios of stationarity in 1,000 *times replications of testing procedure with the realization of Thomas, Poisson and zonal stationary point processes*

Model	number of sub-windows	using 9 frequencies	without $\boldsymbol{\omega}_9$
T(2,1,6)	9	0.128	0.085
T(2,1,8)	9	0.105	0.060
T(5,0.25,4)	9	0.084	0.039
T(5,0.25,6)	9	0.059	0.033
T(5,0.25,8)	9	0.059	0.033
T(5,0.5,4)	9	0.040	0.014
T(5,0.5,6)	9	0.026	0.009
T(5,0.5,8)	9	0.037	0.017
T(5,1,4)	9	0.016	0.006
T(5,1,6)	9	0.013	0.005
T(5,1,8)	9	0.002	0.001
T(7,0.25,4)	9	0.042	0.019
T(7,0.25,6)	9	0.033	0.013
T(7,0.25,8)	9	0.023	0.015
T(7,0.5,4)	9	0.017	0.003
T(7,0.5,6)	9	0.013	0.005
T(7,0.5,8)	9	0.006	0.001
T(7,1,4)	9	0.004	0.003
T(7,1,6)	9	0.000	0.001
T(7,1,8)	9	0.000	0.000
P(20)	9	0.003	0.001
P(30)	9	0.000	0.000
P(50)	9	0.000	0.000
y	9	0.999	0.999
ZSI	9	1.000	1.000
ZSI	4	0.994	0.993
$ZSII$	9	0.999	1.000
$ZSII$	4	0.979	0.985

existing points and the new point is smaller than r, then the newly-generated point is eliminated and another random point is generated. The empirical power of test is close to one for the point pattern y. In order to obtain the empirical power of test, two other zonal stationary point patterns are generated on a rectangular window $W = [0, 70]^2$. Both zonal stationary point patterns consist of four local stationary point patterns observed on regular square sub-regions of W as follow:

- Zonal stationary I (ZSI): In three sub-windows out of four, realizations of $T(0.0163, 1, 4)$ are considered and the remained sub-window contains a realization of $SSI(3)$.
- Zonal stationary II (ZSII): In two sub-windows, realizations of $T(0.0184, 1, 4)$, and in the remained sub-windows realizations of $SSI(2)$ and $P(0.0735)$ are considered.

For both above-mentioned zonal stationary point patterns the considered test is carried out by taking into account 2^2 and 3^2 sub-windows. By considering 2^2 sub-windows, $h = 3$ and $\rho = 34$ are taken into account which returns $\sigma^2 = 0.0138$. The frequencies $\boldsymbol{\omega}_j, j = 1\ldots, 9$ are considered as before but $\mathbf{z}_i$ are chosen as the midpoints of four sub-windows as $\mathbf{z}_1 = (70/4, 70/4)$, $\mathbf{z}_2 = (3 \times 70/4, 70/4)$, $\mathbf{z}_3 = (70/4, 3 \times 70/4)$ and $\mathbf{z}_4 = (3 \times 70/4, 3 \times 70/4)$. For this set of locations and frequencies, we have $df_L = 3$, $df_F = 8$ and $df_{IEr} = 24$. The test procedure is similar to the case where the observation window is partitioned into 3^2 sub-windows. The empirical power of test is close to one in all the zonal stationary cases.

Since the value of the periodogram at higher frequencies can be taken as the contribution of random errors only, so we ignore $\boldsymbol{\omega}_9 = (15\pi/20, 15\pi/20)$ (the frequency with the highest norm) and perform the test by considering $\boldsymbol{\omega}_1, \ldots, \boldsymbol{\omega}_8$. Therefore, we have $df_F = 7$ and $df_{IEr} = 7df_L$. The results of Table 1 show that the empirical size of test decreases when $\boldsymbol{\omega}_9$ is removed from the set of considered frequencies. This means that some parts of information are killed by putting $\boldsymbol{\omega}_9$ aside.

4.1 Real data

4.1.1 Trees data

As mentioned earlier, the first dataset is devoted to the locations of *Euphorbiaceae* trees, as shown in Figure 1. First of all, we use Guan's KPSS test ([11]) to examine the first-order stationarity of this point pattern. From the empirical

Table 2. Analysis of variance table for the trees data

Item	df	SS	$\chi^2(=SS/\sigma^2)$
Between spatial locations	3	0.18	12.74
Between frequencies	8	11.60	838.00
Interaction + residual	24	0.37	26.60
Total	35	12.14	877.34

pair correlation function plot, the dependency appears to be ignorable after $m_n = 5$. The resulting Guan's test statistic is equal to 0.1607, which is smaller than the critical value at level of 0.05 (≈ 0.3244). Thus, it is concluded that this point pattern is first-order stationary and we can then proceed our test. Postulating that all of the assumptions made in Section 4 are valid for this case, we consider $h = 3$ and $\rho = 34$. Thus, the distance between the locations $\mathbf{z}_i$ and frequencies $\boldsymbol{\omega}_j$ points must be at least 34 and $\pi/3$, respectively, and the value of σ^2 will be equal to $16h^2/(9\rho^2) \approx 0.0138$. The points $\mathbf{z}_1, \ldots, \mathbf{z}_4$ are the centroids of the four equally-dimensioned subregions denoted by $\mathbf{S}_1, \ldots, \mathbf{S}_4$ from left to right and down to up, respectively. More precisely, the points $\mathbf{z}_i$ are chosen as $\mathbf{z}_1 = (70/4, 70/4)$, $\mathbf{z}_2 = (3 \times 70/4, 70/4)$, $\mathbf{z}_3 = (70/4, 3 \times 70/4)$, and $\mathbf{z}_4 = (3 \times 70/4, 3 \times 70/4)$. We denote the restricted point patterns to $\mathbf{S}_1, \ldots, \mathbf{S}_4$ by $\mathbf{x}_1, \ldots, \mathbf{x}_4$, respectively. The number of observed trees at the regions $\mathbf{S}_1, \ldots, \mathbf{S}_4$ are almost the same. Firstly, we consider the estimate of K function for investigating the inter-point dependence aspects of these point patterns. The sample K functions of each point pattern along the theoretic K function of the stationary Poisson process are shown in Figure 7. Simply speaking, the gray areas of all the figures represent the acceptance regions of the stationary Poisson model for data. The hypothesis of stationary Poisson model will be rejected at level of $\alpha = 0.05$, when the sample statistic does not remain between the given boundaries at least for a point $r \in \mathbb{R}_+$. When the sample K functions compared with the prepared boundaries, the lack of fitness of stationary Poisson process to all of the point patterns is emphasized. Visually, the sample K functions of all the point patterns except $\mathbf{x}_2$ are approximately the same. In the following, we apply our proposed method to test the nonstationarity of this point pattern. Afterwards, if the test rejects the stationarity assumption against the zonal stationarity, then we use the post-hoc tests for detecting the location(s) at which the structure of trees pattern is changed.

Table 2 presents the results of the analysis of variance for this setting of locations and frequencies using the logarithm of local periodogram. The interaction term is not significant (χ^2 is small compared to $\chi^2_{24}(0.05) = 36.42$) confirming that the point pattern is uniformly modulated. Moreover, both 'between spatial locations' and 'between frequencies' sums of squares are highly significant ($SSL/\sigma^2 > \chi^2_3(0.05) = 7.81$ and $SSF/\sigma^2 > \chi^2_8(0.05) = 15.51$), suggesting that the point pattern is nonstationary and the spectra are nonuniform. The analysis of variance indicates a significant difference in

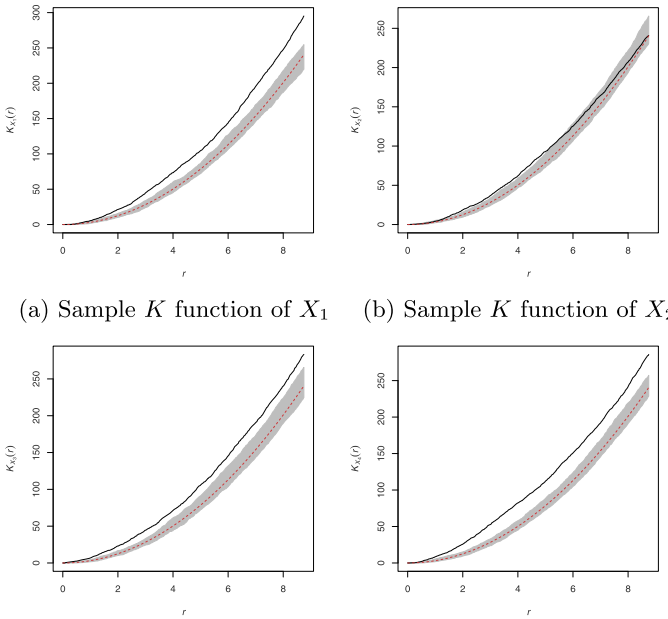

(a) Sample K function of X_1 (b) Sample K function of X_2

(c) Sample K function of X_3 (d) Sample K function of X_4

Figure 7. The estimated K function for trees data computed for point patterns restricted in square windows with centers $\mathbf{z}_1, \ldots, \mathbf{z}_4$ and the resulting point process is mentioned by $X_1, \ldots, X_4$, respectively. The figures contain the sample K functions (solid line), the theoretic functions for the stationary Poisson point process (dashed red line), and upper and lower boundaries based on the enveloping of 99 simulations from stationary Poisson process (gray area).

the locations effect. Thus, we use the Bonferroni method for multiple comparisons to discover different locations. There is a set of $\binom{4}{2} = 6$ hypotheses to test, say, $\alpha_i = \alpha_j$ for $i \neq j$ and $i, j = 1, \ldots, 4$. The Bonferroni method rejects each test if $SSL/\sigma^2 > \chi^2_1(\alpha/6)$. The Bonferroni method simply reduces the significance level of each individual test so that the sum of the significance levels is no greater than α.

Table 3 shows the results of post-hoc tests. There is a significant difference between the local periodograms at locations $\mathbf{z}_2$ and $\mathbf{z}_4$, while the behavior of the local periodograms does not change at other locations. Since the numbers of observed trees in both areas ($\mathbf{S}_2$ and $\mathbf{S}_4$) are almost the same, the difference between the local periodograms at locations $\mathbf{z}_2$ and $\mathbf{z}_4$ may be due to the significance of the latitude effect on the competition between trees.

4.1.2 Capillaries data

The stationary Strauss hard-core model was suggested for the locations of capillaries in prostate tissues [17, 18]. It has been concluded that capillary profile patterns are more clustered in healthy tissue than those of cancerous tissue. The difference in the spatial model of healthy and cancerous tissues has been also verified [13] by testing the

Table 3. The Bonferroni post-hoc test for the trees data

Item	df	$\chi^2(=SS/\sigma^2)$ statistic	p-value
$\mathbf{z}_1$ vs $\mathbf{z}_2$	1	1.38	0.24
$\mathbf{z}_1$ vs $\mathbf{z}_3$	1	0.12	0.73
$\mathbf{z}_1$ vs $\mathbf{z}_4$	1	4.99	0.03
$\mathbf{z}_2$ vs $\mathbf{z}_3$	1	0.69	0.41
$\mathbf{z}_2$ vs $\mathbf{z}_4$	1	11.64	$< 0.05/6 = 0.008$*
$\mathbf{z}_3$ vs $\mathbf{z}_4$	1	6.66	0.01

Table 4. Analysis of variance table for the Capillaries data

Healthy tissue			
source of variation	*df*	*SS*	$\chi^2(=\mathrm{SS}/\sigma^2)$
Between spatial locations	3	0.21	15.00
Between frequencies	8	2.77	200.03
Interaction + residual	24	0.39	27.84
Total	35	3.36	242.87
Cancerous tissue			
source of variation	*df*	*SS*	$\chi^2(=\mathrm{SS}/\sigma^2)$
Between spatial locations	3	0.53	38.20
Between frequencies	8	1.90	136.94
Interaction + residual	24	0.25	17.96
Total	35	2.67	193.09

corresponding empirical K functions. The intensities of two point patterns are almost the same. According to the stationarity assumption of these point patterns considered by [17, 18], the second order properties of healthy and cancerous tissues have been compared by [27] concluding that cancer does not affect the first and second order properties of the locations of capillaries on the prostate tissue. These researches have assumed the corresponding point process to be stationary. Here, we apply our proposed method to test the zonal stationarity of both point patterns. The observation windows are rescaled to $[0, 70]^2$ squares and all the required values are assumed to be same as the previous settings.

The results of the analysis of variance and post-hoc test for this dataset are presented at Table 4 and 5, respectively. The results show that the effect of location is significant for both of the healthy and cancerous point patterns. According to the new obtained evidence, the previous results can not be invoked. Nevertheless, we can use the local periodograms to extend the idea of [27] for comparing the spectral density functions of nonstationary point patterns. The asymptotic independence and the asymptotic distribution of local periodograms are used to compute the density function of the local periodograms and hence the likelihood function in terms of the local periodograms similar to [27]. Let $I^{\mathrm{h}}_{\mathbf{z}_i}(\boldsymbol{\omega}_j)$ denotes to the local periodogram of healthy point pattern at the location $\mathbf{z}_i$ and frequency $\boldsymbol{\omega}_j$ and there is similar notation, i.e., $I^{\mathrm{c}}_{\mathbf{z}_i}(\boldsymbol{\omega}_j)$, for cancerous one. Thus, the likelihood ratio for comparing the local spectral density functions of two independent point patterns at the location $\mathbf{z}_i$ is

Table 5. The Bonferroni post-hoc test for the Capillaries data. The significant differences in the location effects are denoted by '*'

Healthy tissue			
test	*df*	$\chi^2 = SS/\sigma^2$	p-value
$\mathbf{z}_1$ vs $\mathbf{z}_2$	1	4.65	0.03
$\mathbf{z}_1$ vs $\mathbf{z}_3$	1	13.94	$< 0.05/6 = 0.008$*
$\mathbf{z}_1$ vs $\mathbf{z}_4$	1	7.60	0.006*
$\mathbf{z}_2$ vs $\mathbf{z}_3$	1	2.49	0.11
$\mathbf{z}_2$ vs $\mathbf{z}_4$	1	0.36	0.55
$\mathbf{z}_3$ vs $\mathbf{z}_4$	1	0.95	0.33
Cancerous tissue			
test	*df*	$\chi^2 = SS/\sigma^2$	p-value
$\mathbf{z}_1$ vs $\mathbf{z}_2$	1	18.53	$< 0.05/6 = 0.008$*
$\mathbf{z}_1$ vs $\mathbf{z}_3$	1	32.45	< 0.008*
$\mathbf{z}_1$ vs $\mathbf{z}_4$	1	22.35	< 0.008*
$\mathbf{z}_2$ vs $\mathbf{z}_3$	1	1.94	0.16
$\mathbf{z}_2$ vs $\mathbf{z}_4$	1	0.18	0.67
$\mathbf{z}_3$ vs $\mathbf{z}_4$	1	0.94	0.33

$$\Lambda_{\mathbf{z}_i} = \prod_{j=1}^{9} \frac{4 I^{\mathrm{h}}_{\mathbf{z}_i}(\boldsymbol{\omega}_j) I^{\mathrm{c}}_{\mathbf{z}_i}(\boldsymbol{\omega}_j)}{(I^{\mathrm{h}}_{\mathbf{z}_i}(\boldsymbol{\omega}_j) + I^{\mathrm{c}}_{\mathbf{z}_i}(\boldsymbol{\omega}_j))^2}.$$

Finally, the resulting likelihood ratio is compared with 0.025 and 0.975 quintiles estimated using the simple Monte Carlo simulation. The values of $\Lambda_{\mathbf{z}_i}, i = 1, ..., 4$ are $0.93, 0.95, 0.89$ and 0.94, respectively, and the estimated quintiles are 1.07×10^{-5} and 0.20. The results of likelihood ratio test show that there are significant differences between the local spectral density functions of healthy and cancerous point patterns at the locations $\mathbf{z}_i, i = 1, ..., 4$. Therefore, assuming the nonstationarity of both point patterns, we can conclude that cancer affects the second order structure of prostate tissue. This means that although the number of capillaries and their aggregation have not been affected by cancer, the interaction of the location of capillaries is reflected on the changes in the tissue structure.

ACKNOWLEDGEMENTS

The authors would like to express their gratitude to the anonymous referees for interesting and helpful comments that revolutionary improved the previous version of this paper.

Received 28 January 2017

REFERENCES

[1] Bandyopadhyay, S. and Lahiri, S. (2009). Asymptotic properties of discrete fourier transforms for spatial data. *Sankhyā: The Indian Journal of Statistics, Series A* 221–259. MR2639292

[2] Bandyopadhyay, S. and Rao, S. S. (2016). A test for stationarity for irregularly spaced spatial data. *J. Roy. Statist. Soc. Ser. B (Statistical Methodology)*. MR3597966

[3] Bartlett, M. S. (1964). The spectral analysis of two-dimensional point processes. *Biometrika* **51** 299–311. MR0175254

[4] Besag, J. (1977). Contribution to the discussion of Dr. Ripley's paper. *J. Roy. Statist. Soc. Ser. B* **39** 193–195. MR0488279
[5] Chiu, S. N. and Liu, K. I. (2013). Stationarity tests for spatial point processes using discrepancies. *Biometrics* **69** 497–507. MR3071068
[6] Dahlhaus, R. (1996). Asymptotic statistical inference for non-stationary processes with evolutionary spectra. In *Athens Conference on Applied Probability and Time Series Analysis, Vol. II (1995). Lecture Notes in Statist.* **115** 145–159. Springer, New York. MR1466743
[7] Diggle, P. J. (1983). *Statistical analysis of spatial point patterns. Mathematics in Biology*. Academic Press, Inc. [Harcourt Brace Jovanovich, Publishers], London. MR743593
[8] Fuentes, M. (2001). A New High Frequency Kriging Approach for Nonstationary Environmental Process. *Environmetrics* **12** 469–483.
[9] Fuentes, M. (2002). Modeling and prediction of nonstationary spatial processes. *Statistical Modeling* **9** 281–298.
[10] Fuentes, M. (2005). A formal test for nonstationarity of spatial stochastic processes. *J. Multivariate Anal.* **96** 30–54. MR2202399
[11] Guan, Y. (2008). A KPSS test for stationarity for spatial point processes. *Biometrics* **64** 800–806. MR2526630
[12] Guyon, X. (1982). Parameter estimation for a stationary process on a d-dimensional lattice. *Biometrika* **69** 95–105. MR655674
[13] Hahn, U. (2012). A studentized permutation test for the comparison of spatial point patterns. *Journal of the American Statistical Association* **107** 754–764. MR2980082
[14] Hawkes, A. G. (1971). Spectra of some self-exciting and mutually exciting point processes. *Biometrika* **58** 83–90. MR0278410
[15] Jenkins, G. M. (1961). General considerations in the analysis of spectra. *Technometrics* **3** 133–166. MR0125731
[16] Kim, H.-M., Mallick, B. K. and Holmes, C. C. (2005). Analyzing nonstationary spatial data using piecewise Gaussian processes. *J. Amer. Statist. Assoc.* **100** 653–668. MR2160567
[17] Mattfeldt, T., Eckel, S., Fleischer, F. and Schmidt, V. (2006). Statistical analysis of reduced pair correlation functions of capillaries in the prostate gland. *Journal of microscopy* **223** 107–119. MR2247180
[18] Mattfeldt, T., Eckel, S., Fleischer, F. and Schmidt, V. (2007). Statistical modelling of the geometry of planar sections of prostatic capillaries on the basis of stationary Strauss hard-core processes. *Journal of microscopy* **228** 272–281. MR2412516
[19] Mø ller, J. and Waagepetersen, R. P. (2004). *Statistical inference and simulation for spatial point processes. Monographs on Statistics and Applied Probability* **100**. Chapman & Hall/CRC, Boca Raton, FL. MR2004226
[20] Mugglestone, M. A. and Renshaw, E. (1996). A practical guide to the spectral analysis of spatial point processes. *Comput. Statist. Data Anal.* **21** 43–65. MR1380832
[21] Priestley, M. (1967). Power spectral analysis of non-stationary random processes. *Journal of Sound and Vibration* **6** 86–97.
[22] Priestley, M. B. (1965). Evolutionary spectra and non-stationary processes.(With discussion). *J. Roy. Statist. Soc. Ser. B* **27** 204–237. MR0199886
[23] Priestley, M. B. (1966). Design relations for non-stationary processes. *J. Roy. Statist. Soc. Ser. B* **28** 228–240. MR0199943
[24] Priestley, M. B. and Subba Rao, T. (1969). A test for non-stationarity of time-series. *J. Roy. Statist. Soc. Ser. B* **31** 140–149. MR0269062
[25] Renshaw, E. and Ford, E. D. (1983). The Interpretation of Process from Pattern Using Two-Dimensional Spectral Analysis: Methods and Problems of Interpretation. *J. Roy. Statist. Soc. Ser. B.* **32** 51–63.
[26] Ripley, B. D. (1976). The second-order analysis of stationary point processes. *J. Appl. Probability* **13** 255–266. MR0402918
[27] Saadatjouy, A. and Taheriyoun, A. (2016). Comparing the second-order properties of spatial point processes. *Statistics And Its Interface* **9** 365–374. MR3457503
[28] Stoyan, D. and Stoyan, H. (1996). Estimating pair correlation functions of planar cluster processes. *Biometrical Journal* **38** 259–271.
[29] Zhang, T. and Zhou, B. (2014). Test for the first-order stationarity for spatial point processes in arbitrary regions. *J. Agric. Biol. Environ. Stat.* **19** 387–404. MR3292563

Azam Saadatjouy
Department of Statistics,
Shahid Beheshti University, G.C.
Evin, 1983969411, Tehran, Iran.
E-mail address: a_saadatjouy@sbu.ac.ir

Ali Reza Taheriyoun
Department of Statistics,
Shahid Beheshti University, G.C.
Evin, 1983969411, Tehran, Iran.
E-mail address: a_taheriyoun@sbu.ac.ir

Mohammad Q. Vahidi-Asl
Department of Statistics,
Shahid Beheshti University, G.C.
Evin, 1983969411, Tehran, Iran.
E-mail address: m-vahidi@sbu.ac.ir